Quantification of Magnetic Resonance Spectroscopy signals with lineshape estimation

M.I Osorio-Garcia[a], D.M Sima[a], F.U Nielsen[b], U. Himmelreich[b], and S. Van Huffel[a]

[a]Dept. Electrical Engineering - ESAT-SCD, Katholieke Universiteit Leuven

[b]Biomedical Nuclear - Magnetic Resonance Unit, Katholieke Universiteit Leuven

Abstract

Quantification of Magnetic Resonance Spectroscopy (MRS) signals is required for providing metabolite concentrations of the tissue under investigation. For estimating these concentrations several biochemical and acquisition conditions need to be taken into account. Until now it is still a challenge to obtain reliable concentrations as experimental conditions may have a detrimental effect on the spectral quality. The lineshape of MRS signals is affected, for instance, by inhomogeneities of the static magnetic field arising from imperfect shimming and tissue heterogeneities. To handle this type of distortions, we propose an extension of the self-deconvolution method, where a common lineshape is estimated and a robust method with local regression is included to improve the smoothing of the estimated damping (or lineshape) function. This common lineshape is imposed in the metabolite quantification method and the spectral parameters (amplitude, frequency, damping and phase corrections) are obtained via nonlinear least squares. In this study, we considered distorted simulated, *in vitro* and *in vivo* rat brain signals which were lineshape corrected and quantitative results were compared in all three cases.

Keywords: Magnetic Resonance Spectroscopy (MRS); lineshape; shimming; quantification

1 Introduction

Quantification of Magnetic Resonance Spectroscopy (MRS) signals can be used for the diagnosis of cancer, epilepsy, metabolic and other diseases, because it provides in a non-invasive way the concentration of metabolites, which reflect the biochemical conditions of a tissue under investigation. Several quantification methods in the time and frequency domain have been developed for this purpose [21, 22, 24, 25]. MRS signals are characterized by relatively low signal-to-noise ratio (SNR), overlapping resonances, underlying macromolecules and lipids and a baseline affecting the signal.

MRS signals are measured in the time domain and are composed of a sum of decaying complex-valued sinusoids containing information about metabolites. By transforming to the frequency domain we obtain a spectrum composed of a series of peaks corresponding to these metabolites. The lineshape of each peak is ideally of a Lorentzian type, corresponding in the time domain to an exponentially decaying sinusoid. In the frequency domain this yields a spectral line with homogeneous broadening. However, when magnetic field perturbations, field inhomogeneities or tissue heterogeneities are present, these lineshapes are disturbed (in symmetry and linewidth) and make the fitting of the signal using an ideal lineshape (*e.g.* Lorentzian or Gaussian) unreliable or tending to mislead the metabolite estimates. Especially in *in vivo* MRS, unwanted distortions may affect the natural Lorentzian lineshape of resonances in the signal. Such a lineshape is determined by the dampings of the time domain signal, which might not be pure decaying exponentials. Some of the lineshape problems are related to faster relaxation (*i.e.*, when the external local magnetic field is not ideally homogeneous, this produces a smaller effective relaxation time T_2^*), low SNR, inhomogeneities caused by the magnet design, tissue inhomogeneities, variations in the tissue type or paramagnetic material inside the bore, such as dental materials in filling, crowns, metallic dental implants and head holders. Hence, *in vivo* measurements, *e.g.*, from the human brain, are more susceptible to sample heterogeneities compared to *in vitro* signals.

The lineshape problem has been studied using different approaches which require corrections during [2, 8, 10, 11] or subsequent to [1, 7, 12, 17, 18, 20, 27, 28, 32] MRS acquisition. Methods in the first category are called shimming techniques, and are applied during the MR scanning

session in order to try to correct field inhomogeneities and thus improve spectral quality. MRS acquisitions at high magnetic fields exhibit lineshape distortions that may only be corrected using higher-order shimming techniques, which are not always available [8, 9, 14]. Moreover, because of local magnetic field susceptibility problems (*e.g.*, measurements near an air cavity such as sinuses), shimming can not always compensate for local field inhomogeneities, and the lack of spectral quality leads to lineshape distortions.

Studies on lineshape correction during signal post-processing aim at enhancing the spectral resolution of *in vivo* ^{1}H MRS based on the deconvolution of spectra using as reference the lineshape derived from a reference signal [1, 12, 18, 32], but there exist also several reference-free methods that extract a common lineshape by modelling the signal itself [17, 20, 23, 27, 28] or by magnetic field mapping [7].

Reference deconvolution methods such as the one presented in [18, 32], can successfully correct for lineshape distortions but require the use of a separate reference acquisition signal or a well-separated reference line, which is part of the spectrum of interest. For ^{1}H MRS the water signal is used as reference, however, limitations related to extra acquisitions or incorrect reference signal limit its application. On the other hand, when targeting other nuclei rather than ^{1}H, the lineshape estimation becomes more important because no water reference is available. The overlapping of resonances due to low magnetic field strength is also another limitation when using reference deconvolution methods, because then a clear separation of a reference peak is not possible.

Methods that do not use a reference signal, [17, 20, 23, 27, 28], also require that all resonances of interest have the same lineshape, thus they have a common distortion that can be assumed to be similar for all metabolites within a measurement. These methods involve the incorporation of non-parametric models for modelling the lineshape using exponential functions, polynomials, sinusoids, wavelets or splines, implying the adjustment of certain hyper-parameters for those specific functions. For instance, Provencher [23], uses a balance between over-parameterization and over-simplification of the baseline and lineshape parameters by using a complex regularization scheme. In [28], Slotboom *et al.* models the lineshape together with the regular model parame-

ters, thus the lineshape is modelled as a sum of weighted Dirac delta functions in the frequency domain.

In this paper, we extend the study and improve the lineshape estimation algorithm proposed by [27]. Sima *et al.* [27] showed that lineshape estimation by self-deconvolution is applicable to short-echo time MRS signals by imposing a calculated lineshape to the metabolite profiles in the quantification algorithm AQSES [21]. In [27], the lineshape estimation method has only been evaluated on simulated MRS signals, which were constructed from a basis set of metabolite profiles and then distorted with an asymmetrical lineshape. Here, we investigate the lineshape correction for more complex mis-shimmed spectra originating not only from simulated signals, but also from acquired *in vitro* and *in vivo* signals. For the measured signals, the lineshape was deliberately distorted by deteriorating the shim quality, thus simulating some common distortions of real MRS signals. To respond to the increased complexity of measured signals, the lineshape modelling methods analyzed in [27] are replaced here by a smoothing method using robust local regression.

Furthermore, *in vivo* short-echo time ^{1}H MRS signals also contain high contributions from macromolecules (MM) and lipids affecting their natural flat baseline. The main feature of this background signal is the line broadening arising from lipids and macromolecular components which overlap with the narrower peaks of metabolites. This baseline may be either measured *in vivo* using an inversion recovery approach (metabolite nulled signal that contains only macromolecular components) [6, 13], it can be estimated from the first points of the time domain signal (which contain fast relaxation components such as macromolecules and lipids), or it can be computed using signal processing techniques that model it non-parametrically via splines, polynomials or wavelets [5, 6, 21, 22, 24–26]. The new method presented in this paper also takes into account the presence of macromolecules and lipids in the *in vivo* rat brain signals.

2 Materials and Methods

2.1 MRS signals

All MR *in vitro* and *in vivo* data were acquired on a 9.4 Tesla (T) Bruker Biospec small animal MR scanner (Bruker BioSpin MRI, Ettlingen, Germany) with a magnet bore of 20 cm using a 7 cm linear body resonator as transmitter combined with a circular polarized ^{1}H rat brain surface coil for signal reception. *In vitro* and *in vivo* Single Voxel Spectroscopy (SVS) spectra were obtained using the PRESS pulse sequence [3] with implemented pre-delay outer volume suppression as well as the water suppression method, VAPOR [31]. MRS parameters were: TR=8s, TE=20ms, SW=4KHz and 128 averages. Spectra were corrected for B_0 instability due to eddy currents as well as B_0 drift using the Bruker built-in routines. Remaining shimming problems, line broadening and non-Lorentzian character of the peaks may still be present after correcting for eddy currents. Shimming was performed using FASTMAP [8]. SVS and FASTMAP Volumes of Interest (VOI) were 4x4x4 mm^3. The VOI was positioned close to the magnet iso-center and almost in the middle of the phantom containing the metabolites. The VOI for the *in vivo* measurements was placed on the right hemisphere of the thalamus.

- **Basis set of reference metabolites.** We obtained a basis set of metabolites from 50 mM solutions of Alanine (Ala), Aspartate (Asp), Creatine (Cre), Gamma-Aminoburytic acid (GABA), Glucose (Glc), Glutamine (Gln), Glutamate (Glu), Glycerolphosphorylcholine (GPC), Glutathione (GSH), Lactate (Lac), Myo-Inositol (m-Ins), N-Acetyl Aspartate (NAA), Phosphorylcholine (PCh), Phospocreatine (PCr), Phosphoryl Ethanolamine (PE) and Taurine (Tau). Metabolites were dissolved in Phosphate Buffer Solution (PBS) and 5 mM DSS was added as a chemical shift reference. GPC and PCh were dissolved in 100 mM NaCl containing 5 mM Trimethylsilylpropanesulfonic acid sodium salt (DSS). pH for every phantom was adjusted to 7.20$\pm$0.10. NMR acquisition parameters were as described above, but with 64 averages and no B_0 drift correction. The basis set of reference metabolites is shown in Fig.1.

- **Simulated signals.** Generation of simulated signals was performed in Matlab® (The Math-

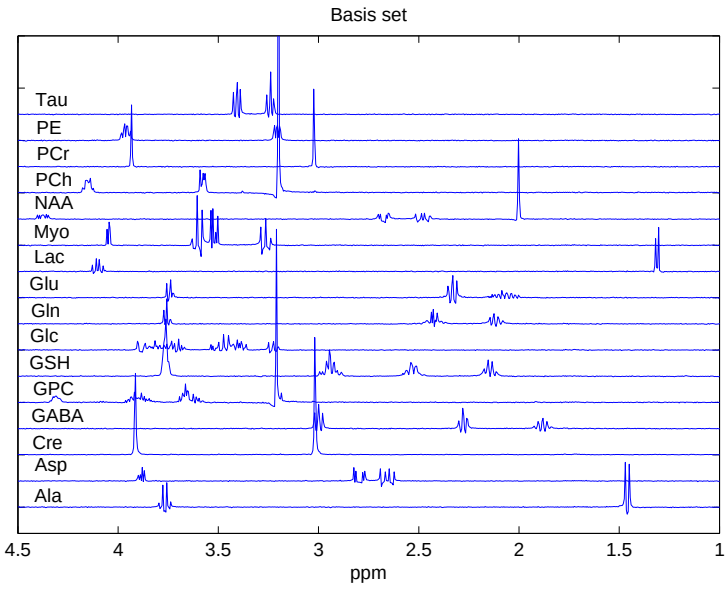

Figure 1: Spectra of the metabolite basis set measured *in vitro* at 9.4 T. Acquisition parameters: PRESS sequence, TR=8s, TE=20ms, SW=4KHz and 64 averages.

works ™). We created a simulated MRS signal $(y_m(t))$ composed of 7 *in vitro* measured metabolites from the basis set described above: Ala, Cre, Gln, Glu, Lac, NAA, and Tau. The MRS signal was generated by summing up the signals of all 7 metabolites, then a distortion was included to simulate a damping different from the ideal Lorentzian.

$y_m(t)$ was point-wise multiplied by a damping function $D(t) = A(t).e^{i(c_1 e^{\lambda_1 t} + c_2 e^{\lambda_2 t})}$, where $\lambda_1, \lambda_2 < 0$, $i = \sqrt{-1}$ and $A(t)$ is the Fourier Transform of an asymmetric triangular shape,

$$A(t) = \frac{1}{2(f_3 - f_1)} . \frac{1}{2\pi j t} \left[\frac{e^{x_1} - e^{x_2}}{x_2 - x_1} + \frac{e^{x_3} - e^{x_2}}{x_3 - x_2} \right] \tag{1}$$

where $x_i = 2\pi j f_i t$ for i = 1,2,3 and f_i are the 3 frequencies defining the triangle. See [27] for further details. The second factor of $D(t)$ represents eddy currents in the metal walls of the magnet.

Then the distorted signal $y_d(t)$ becomes:

$$y_d(t) = y_m(t).D(t) + N(t) \tag{2}$$

where $N(t)$ is the added white Gaussian noise.

The white Gaussian noise corresponding to several signal-to-noise ratios (SNRs) is added in the time domain (see Fig.2) and is related to the measured power of the signal in dB, $P_{sig} = 10\log_{10}\frac{\|y_d(t)\|^2}{n}$ (*i.e.* the squared Euclidean norm of the signal divided by the length of the signal, transformed to dB), where the added noise $N(t)$ has standard deviation of:

$$\sigma = \sqrt{10^{\frac{P_{sig}-SNR}{10}}} \tag{3}$$

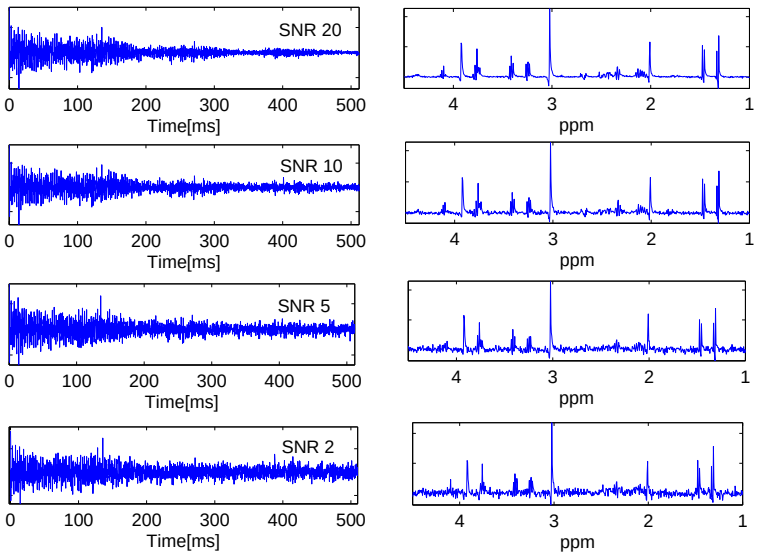

Figure 2: Simulated distorted MRS signal with different SNR levels. The white Gaussian noise is added in the time domain and is related to the measured power of the signal.

The simulated signal with different damping and noise levels is shown in Fig.3.

- ***In vitro* signals.** We obtained a phantom solution containing 5 mM of the following metabolites: Ala, Cre, Gln, Glu, Lac, NAA and Tau, see Fig.4. Metabolites were dissolved in PBS and DSS was added as chemical shift reference at a concentration of 5 mM. The pH of the phantom was adjusted to 7.20$\pm$0.10. After acquiring an undistorted signal with default shimming, the shimming parameters were mis-set by changing the shim current of the X coil generating 2 distorted signals for analysis.

- ***In vivo* signal.** We measured rat brain spectra from the right hemisphere of the thalamus using the measurement conditions described above. Two distorted signals were acquired by mis-setting the shimming parameters, where the Z^2 second order shim coil and the first order X coil values were mis-set (See Fig.5). The SNR of the *in vivo* signals is 12, calculated in the time domain according to Eq.3.

  The baseline of *in vivo* MRS is everything else that can not be assigned to spectra of metabolites, macromolecules or lipids (MM). In this study, the *in vivo* signal from MM was measured using an inversion recovery sequence with a 1ms Hermitian inversion pulse. The inversion time and repetition time were 800 ms and 3 s respectively and 1024 averages were acquired. The inversion time was fine-tuned experimentally for metabolite nulling. Remaining peaks of Cre and Tau were eliminated by filtering the resonances in the time domain using HLSVD-PRO [15] in the post-processing step and the whole spectrum was apodized with a line broadening of 10 Hz. Because MM has a shorter relaxation time, it was excluded when calculating the common lineshape $g(t)$, but it was included in the metabolite basis set for the quantification.

2.2 Quantification

- **Signal processing.** Due to an analog-digital filter incorporated in the Bruker system, a time circular shift of 68 points (a number provided by Bruker) was applied to all *in vitro* and *in vivo* signals using the jMRUI software package [30]. Further processing consisted on filtering out the residual water and the components corresponding to the DSS and buffer solution. To filter without affecting the metabolite resonances, we applied HLSVD-PRO [15].

- **AQSES.** The quantification method used for analyzing the signals was AQSES [21]. This is a time-domain method that uses metabolite profiles to fit the signal under analysis using a nonlinear least squares approach. The basis set can be measured *in vitro* or simulated using quantum mechanics [29, 30]. In this study, we used *in vitro* signals measured under the same conditions as the signals under investigation, as described in section 2.1. An additional signal corresponding to MM was added to the basis set for quantification of the *in*

vivo signals.

AQSES uses the following model that describes the MRS signals under investigation:

$$y(t) = \sum_{k=1}^{K} a_k e^{(j\phi_k)} e^{(-d_k t + 2\pi j f_k t)} v_k(t) + B(t) + \epsilon(t) \tag{4}$$

where $y(t)$ is the experimental signal, K is the number of metabolites, $v_k(t)$ the metabolite signal k in the basis set, a_k the amplitude, ϕ_k the phase shift correction, d_k the damping, f_k the frequency shift due to B_0 inhomogeneity, $B(t)$ is the baseline which in the case of *in vivo* signals is also measured *in vivo* and included in the basis set of metabolites as $v_{K+1}(t)$ and $\epsilon(t)$ denotes white noise with standard deviation σ.

- **AQSES Lineshape.** Given the fact that the volume of interest is supposed to be sufficiently homogeneous for the metabolites to share the same inhomogeneity profile, and no motion or contamination are supposed to be present, the same lineshape distortion is assumed for all components. Thus, for correcting lineshape distortions in the quantification method, we consider a common lineshape for all spectral components in the model of AQSES, except the macromolecular signal measured *in vivo* [27]. The exponential dampings $e^{(-d_k t)}$ in Eq.(4) are then replaced by the common factor $g(t)$, of arbitrary shape, resulting in:

$$y(t) = g(t) \sum_{k=1}^{K} a_k e^{(j\phi_k)} e^{(2\pi j f_k t)} v_k(t) + B(t) + \epsilon(t) \tag{5}$$

The algorithm for lineshape correction is described below:

Step 1 Fitting. First, with a preliminary spectral analysis we quantify the signal assuming ideal lineshape (*i.e.* Lorentzian) to extract the spectral parameters calculated by AQSES: amplitudes, frequencies, phases and dampings. Then the signal is reconstructed from the estimated spectral parameters not taking into account the damping part.

Step 2 Damping. The damping function is computed as the ratio formula for the common damping $g(t)$:

$$g(t) = \frac{y(t) - B(t)}{\sum_{k=1}^{K} a_k e^{(j\phi_k)} e^{(2\pi j f_k t)} v_k(t)} \tag{6}$$

where in the numerator $y(t)$ is the experimental signal and $B(t)$ is the baseline; and in the denominator K is the number of metabolites, $v_k(t)$ the metabolite signal *k* in the basis set, and the amplitudes a_k, frequency shifts f_k and phase shift ϕ_k are estimated from a previous AQSES iteration from **Step 1** or **Step 4**.

Step 3 Smoothing. Improvement of the algorithm comes in the smoothing part. Numerical instability caused by noise and division by small numbers in (6) creates big outliers which are tackled by smoothing $g(t)$. We employ a robust version of local regression using weighted linear least squares with a second degree polynomial (LOESS), which assigns lower weight to outliers in the regression [4]. Thus, we make use of the robust smoothing implementation from Matlab® (*smooth (loess) and (rloess)*).

Initially, we set to zero the tail of $g(t)$ because in MRS signals the information about the damping is contained in the decaying part of the signal. To select the starting (cut-off) point of the tail, we use information from the original signal $y(t)$ and find the point where this signal decays into the noise. First, we calculate the noise standard deviation (σ) using both the time domain and the frequency domain signal; specifically we use a moving window along each signal and σ is set to the smallest standard deviation among all the windows [1]. Secondly, all points of $y(t)$ smaller in absolute value than σ are selected. Due to signal oscillation, the first selected points might not necessarily belong to the noise and therefore they should not be considered as part of the tail. In order to select the cut-off point, we bin these points (as in a histogram) and make use of the K-means clustering function from Matlab® to separate the bins into two classes according to their height. The class with higher average height represents truly noise points, since they reflect high density of selected points lower than σ. Finally, the first point of this class is selected as the cut-off point. This whole procedure is fully automated.

At last, we apply RLOESS and LOESS which require the selection of a smoothing

[1] Typically the standard deviation is calculated either from the last few points of the time domain signal but this could be influenced by 'ghost' echoes, or from a metabolite-free region from the frequency domain signal, but this could be influenced by baseline contamination.

parameter, which in this case, is a percentage of the number of data points. Thus, we allow values between 5 and 30 % and use cross-validation [16] to select the parameters that better fit the damping function. A two-fold cross-validation method was used, where the partitioning was obtained from the even and odd data points of the time domain signal in order to keep the time indexing, which is very essential in MRS signals.

Step 4 Estimate. Spectral analysis is carried out again, point-wise multiplying the original metabolite basis set with the new smoothed function $g(t)$.

Steps 2-4 are repeated until a residual smaller than a chosen threshold is obtained or a convergence of amplitude estimates is reached. The number of iterations is fixed to a maximum of 30; if this number is reached, errors in the basis set or artifacts may affect the fitting causing a big residual or no convergence. Finally, the amplitude estimates are calculated by a final quantification of the signal which allows small damping variations of metabolites additional to the common damping function.

3 Results

We were able to quantify the MRS signals presenting the different lineshape distortions. The following results show the performance of the method according to the type of signal studied:

- **Simulated signals.** In Fig.3, we show the results obtained for the signals with triangular and eddy current distortions. It shows the quantification results at high and low SNR. On the top row we present the results with small damping and on the bottom row the results with big damping. From these results, the residual containing some patterns, correspond to metabolite contributions that were not correctly quantified due to the Lorentzian lineshape model used in AQSES, while AQSES Lineshape shows an improvement that can be attributed to the free lineshape model.

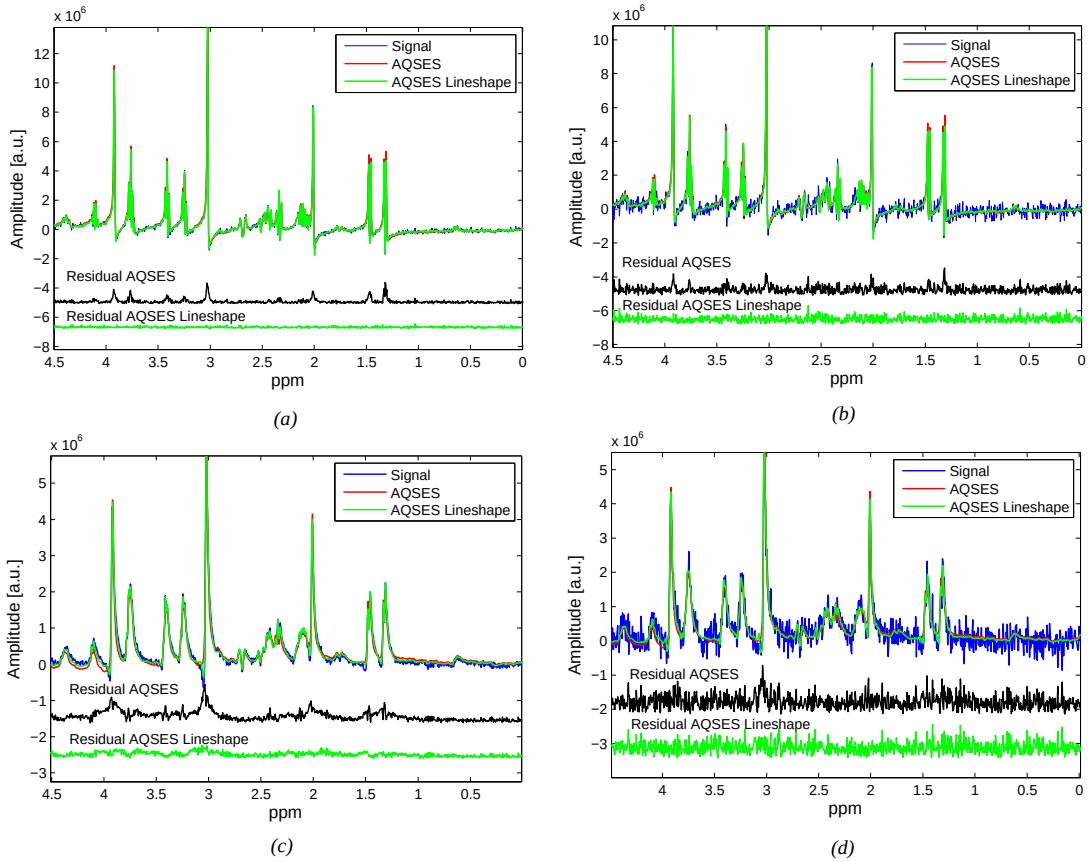

Figure 3: Simulated MRS signals with lineshape distortions and quantification results for different SNR levels and different dampings. These signals are composed of multiple resonances derived from 7 *in vitro* measured metabolites at 9.4 T: Ala, Cre, Gln, Glu, Lac, NAA, and Tau with acquisition parameters: PRESS sequence, TR=8s, TE=20ms, SW=4KHz and 64 averages. Top row: (a) SNR=30, (b) SNR=2 with small dampings (to simulate *in vitro* signals). Bottom row: (c) SNR=20 and (d) SNR=5 with big damping (to simulate *in vivo* signals).

Table I: Mean amplitude estimates and standard deviations for the simulated signals containing 7 metabolites for a set of 100 noise realizations. (a) corresponds to simulated signals with SNR=30 and SNR=2 having small damping (to simulate *in vitro* signals); (b) corresponds to simulated signals with SNR=20 and SNR=5 having big damping (to simulate *in vivo* signals). Results in column 'Original' show amplitude estimates for the undistorted signals quantified with AQSES; while the results in columns 'AQSES' and 'AQSES L' correspond to those of the distorted signals quantified with AQSES and AQSES Lineshape. The true amplitudes are equal to 1 for all metabolites.

Metabolites	SNR 30			SNR 2		
	Original	AQSES	AQSES L	Original	AQSES	AQSES L
Ala	1.0000±0.0025	1.1291±0.0028	1.0124±0.0031	0.9949±0.0732	1.1433±0.0709	1.0353±0.0780
Cre	1.0000±0.001	1.1002±0.0028	1.0162±0.0014	0.9976±0.0274	1.1059±0.0277	1.0125±0.0584
Gln	1.0002±0.004	1.0084±0.0042	1.0058±0.0047	1.0142±0.0960	0.9990±0.1167	0.9968±0.1158
Glu	1.0006±0.0038	1.0555±0.0044	1.0028±0.0048	1.0054±0.1120	1.0733±0.1222	1.0305±0.1184
Lac	1.0000±0.0026	1.1512±0.0027	1.0120±0.0027	1.0001±0.0659	1.1556±0.0627	1.0325±0.0686
NAA	0.9999±0.0022	1.1295±0.0020	1.0171±0.0024	0.9992±0.0499	1.1172±0.0542	0.9987±0.0785
Tau	1.0004±0.0025	1.0678±0.0023	1.0111±0.0024	1.0046±0.0733	1.0670±0.0622	1.0112±0.0666

(a)

Metabolites	SNR 20			SNR 5		
	Original	AQSES	AQSES L	Original	AQSES	AQSES L
Ala	0.9998±0.0464	0.9177±0.0079	0.9536±0.0079	1.0001±0.0464	0.9222±0.0571	0.9663±0.0480
Cre	1.0009±0.0171	1.0111±0.0031	1.0023±0.0049	1.0008±0.0171	1.0129±0.0176	1.0059±0.0248
Gln	0.9933±0.0735	1.0529±0.0122	0.9476±0.0121	0.9946±0.0735	1.0076±0.1027	0.9477±0.0808
Glu	1.0009±0.0647	0.8501±0.0139	1.0098±0.0143	0.9999±0.0647	0.8776±0.0915	1.0185±0.0699
Lac	1.0050±0.0476	0.9191±0.0083	0.9654±0.0088	1.0052±0.0476	0.9257±0.0519	0.9847±0.0547
NAA	1.0048±0.0388	0.9686±0.0074	0.9919±0.0082	1.0048±0.0388	0.9758±0.0396	1.0065±0.0454
Tau	0.9983±0.0349	1.0796±0.0080	1.0202±0.0081	0.9980±0.0349	1.0738±0.0421	1.0140±0.0382

(b)

Table I shows the results of mean amplitude estimates and the corresponding standard deviation for the simulated signal over a set of 100 noise realizations at two SNR levels for small (a) and big damping (b). Results represent the mean amplitude estimates for the original simulated signal quantified with AQSES (with true amplitude 1), the simulated signal with distortions quantified with AQSES and simulated signal with distortions quantified with AQSES Lineshape. Here we observe that the results with AQSES Lineshape are closer to the original values. With high SNR, the variations are very small for both methods, however, the estimates with AQSES are clearly biased from the original expected amplitude estimates. At low SNR there is a higher variation, but the AQSES Lineshape estimates show less bias for the distorted signal.

- ***In vitro* signals.** Results of quantification of *in vitro* signals are shown in Fig.4. The undistorted *in vitro* signal is fitted identically by AQSES and AQSES Lineshape, *i.e.* AQSES Lineshape reports convergence after the first iteration. For the two distorted signals, the resonances of Cre at 3 ppm and 3.9 ppm and the one from NAA at 2 ppm are not very well fitted with AQSES, while AQSES Lineshape is able to accurately fit these peaks. This is due to the fact that the lineshape distortions have a shape different from the typical Lorentzian type considered by AQSES. For both signals in (b) and (c), exhibiting slightly different levels of distortions, we observe similar improvements in the quantification results.

- ***In vivo* signals.** The *in vivo* signals have an additional nuisance to take into account, the macromolecular background signal. In this study, the macromolecular signal was measured by inversion recovery. The undistorted *in vivo* signal is fitted identically by AQSES and AQSES Lineshape, *i.e.* AQSES Lineshape reports convergence after the first iteration. Fig.5 and Fig.6 show the results of quantification and metabolite amplitudes according to the quantification method used. From Fig.5 we could see that the residual using AQSES Lineshape is smaller, on the other hand Fig.6 shows the comparison of amplitude estimates with literature and reveals that there are some metabolites in good agreement while others are under- or overestimated. This effect is much stronger when using AQSES for the distorted signals, which indicates that one should be very careful when evaluating the final results.

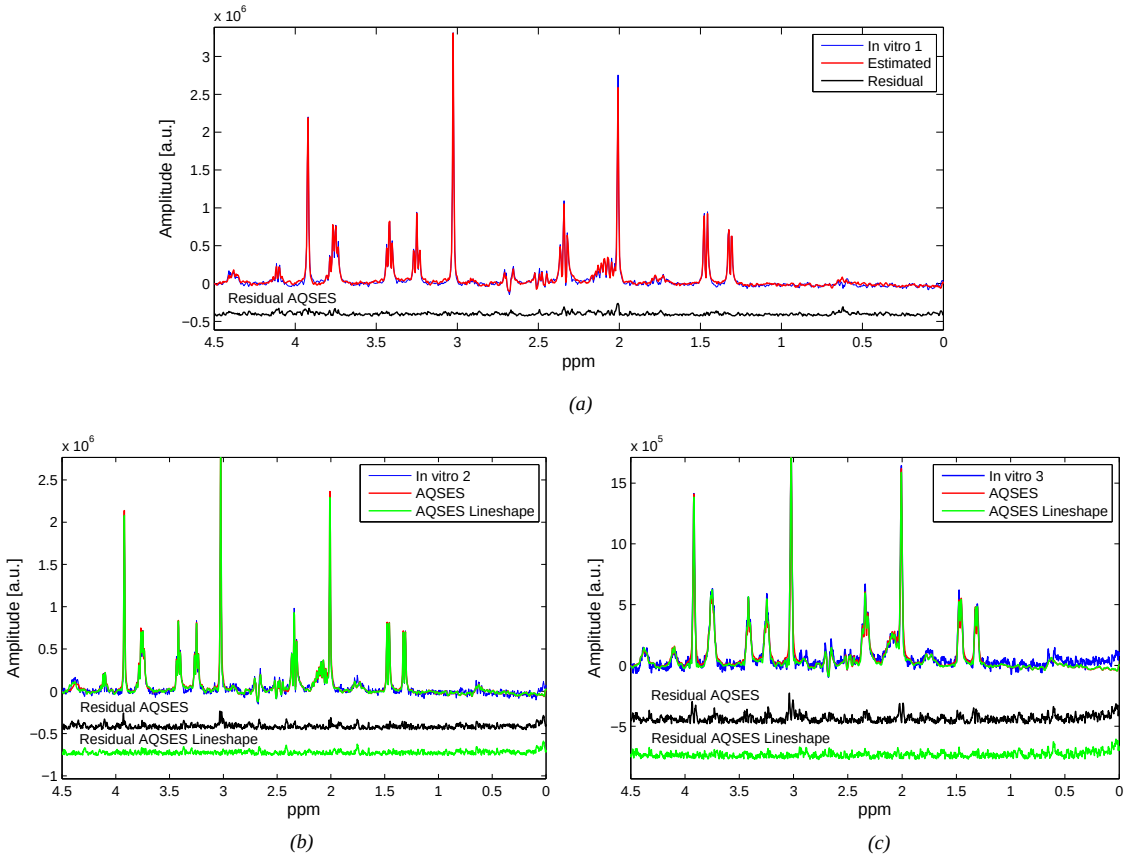

Figure 4: Spectra of *in vitro* MRS signals measured at 9.4 T containing 7 metabolites: Ala, Cre, Gln, Glu, Lac, NAA, and Tau. Acquisition parameters: PRESS sequence, TR=8s, TE=20ms, SW=4KHz and 128 averages. 'In vitro 1' was acquired using the default shimming technique with linewidth=1.36 and SNR=22 (a), then, two distorted signals were acquired by mis-setting the shim current of the X coil: (b) 'in vitro 2' with linewidth=3.92 and SNR=20 and (c) 'in vitro 3' with linewidth=6.52 and SNR=18. (a) was quantified by AQSES; (b) and (c) were quantified by AQSES and AQSES Lineshape.

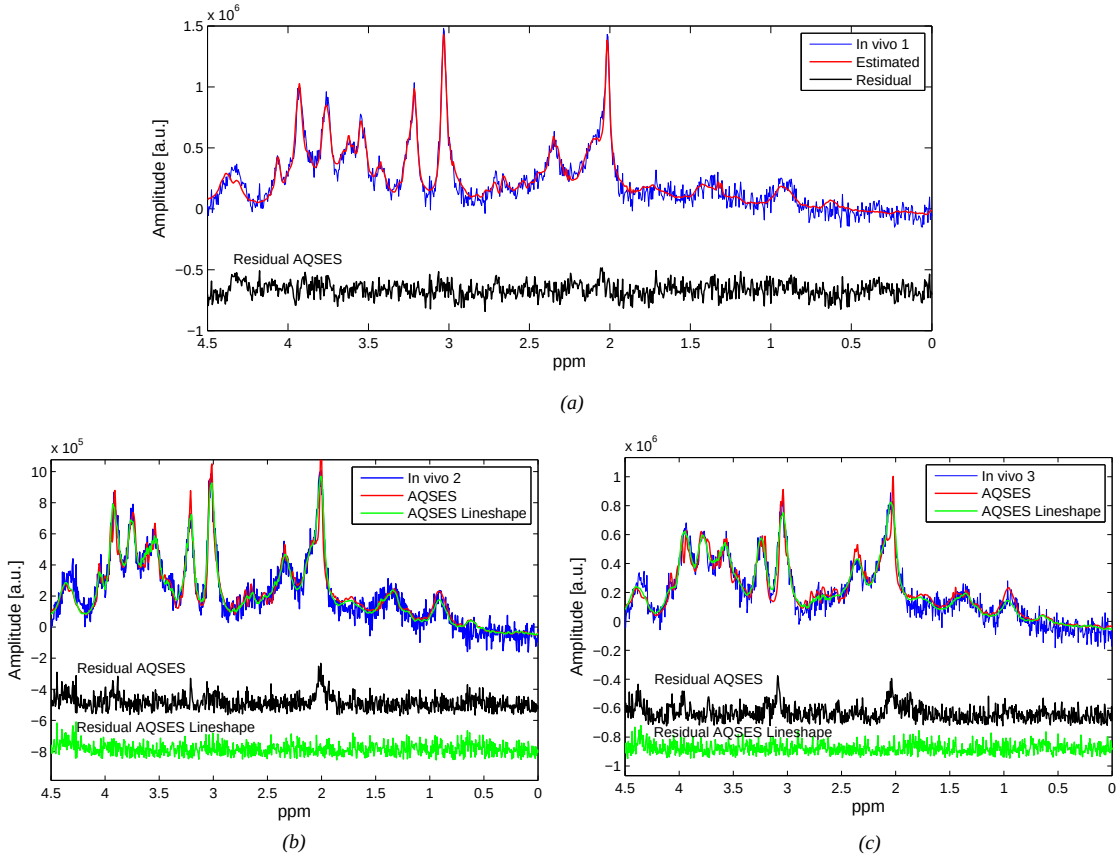

Figure 5: Rat brain *in vivo* spectra from the right hemisphere of the thalamus measured at 9.4 T with acquisition parameters: PRESS sequence, TR=8s, TE=20ms, SW=4KHz and 128 averages. 'In vivo 1' was measured with the default shimming technique, while 'in vivo 2' and 'in vivo 3' were acquired by mis-setting the shimming parameters of the first and second order shim coil X and Z^2. The linewidth for these signals was 17.36, 27.8 and 39.69, respectively with SNR=20. (a) was quantified by AQSES; (b) and (c) were quantified by AQSES and AQSES Lineshape.

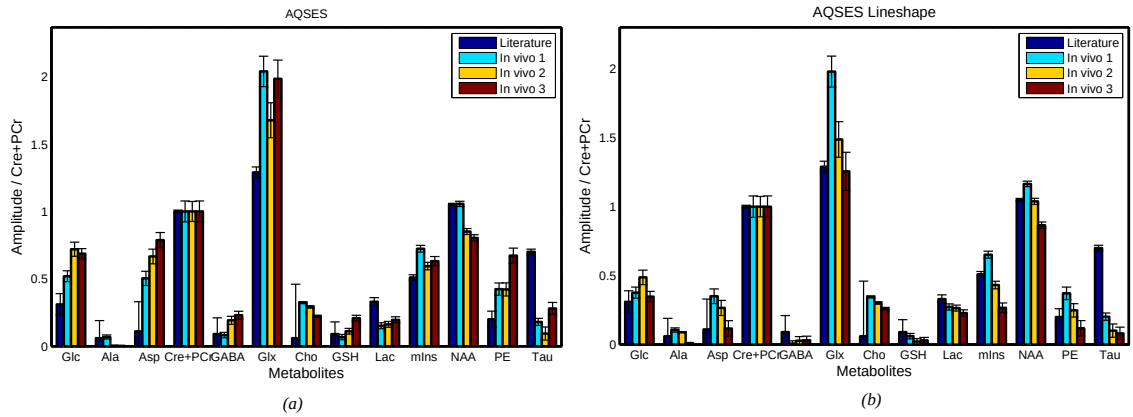

Figure 6: Amplitude estimates for the *in vivo* signal measured at 9.4 T. Results in (a) show amplitude estimates relative to Cre+PCr for the signals quantified with AQSES, and (b) show the results for the signals quantified with AQSES Lineshape. Literature values are obtained from [19]. The error bars on the metabolites correspond to the Cramér-Rao lower bounds.

4 Discussion

MRS signals are ideally composed of Lorentzian lineshapes, however, when magnetic field perturbations, field inhomogeneities or tissue heterogeneities are present, these lineshapes are disturbed (in symmetry and linewidth) and make the fitting of the signal using an ideal lineshape (*e.g.*, Lorentzian or Gaussian) unreliable or tending to mislead the metabolite estimates. As described by several authors [17, 20, 23, 27, 28], one could also estimate the lineshape of MRS signals and include it inside the quantification algorithm.

Other methods might require starting values for estimating the lineshape [28], however, the first iteration on AQSES Lineshape can also be considered as a way to initialize the $g(t)$ function by using the ratio formula followed by fully-automated denoising and further cross-validation is employed for tuning the smoothing criterion. Since none of the current MRS quantification methods uses global optimization techniques, the problem of providing initial values on the parameters is essential for the convergence of local nonlinear least squares methods. Thus, a quantification method that needs as few initial values as possible, and, in fact, implicitly adapts the initial values to the signal under analysis, has practical advantages.

When MRS signals are not heavily distorted it may occur that the Lorentzian lineshape is a good approximation to the shape of the experimental data. AQSES Lineshape works iteratively and evaluates the performance of the quantification after each fit. So the first fit is performed assuming an ideal lineshape (*i.e.* Lorentzian), and then the lineshape is estimated (*i.e.* free model). Finally, in each iteration, residuals of the current and previous fits are compared and the best fit is selected. If the fit using the Lorentzian model is selected, the algorithm will stop after the first iteration.

Quantification of distorted signals with lineshape estimation showed good quantification results for the three types of distorted signals under investigation, thus, simulated, *in vitro* and *in vivo*. The performance of the method was evaluated by validation of amplitude estimates and visual assessment of the residual.

AQSES Lineshape is an automatic method and no user input is required for estimating the lineshape, which is essential for clinical use.

Smoothing. Local regression is an approach of fitting curves to noisy data by a multivariate smoothing procedure, fitting a linear or quadratic function of the predictor variables in a moving fashion, only in a small range of data points similar to how a moving average is computed for a time series. This moving window is also called span. Compared to classical approaches like fitting global parametric functions, local regression substantially increases the type of functions that can be estimated. Another characteristic of local regression is that the methods for making inferences based on local regression fits are nearly the same as those used in parametric fitting. If the function has peaks and valleys, which is the case for the lineshape function, a local linear fit can partially eliminate them, whereas the curvature associated with peaks and valleys is better fit by local quadratic curves. Outliers may strongly influence regression results, but LOESS and RLOESS can iteratively down-weight data points that have large residuals. Concerning the span used during the fitting, we considered a percentage of the data points to be more adequate instead of using a fixed number of points because the number of points in the experimental signals may vary. The size of this span parameter has an important effect on the fitting, thus a span that is

too small leads to a large number of windows denoising the data, providing little smoothing and rather a function characterized by noise with a large variance. On the other hand, if the span is too large, the regression will be over-smoothed and the local polynomial may not fit well the data, resulting in loss of important information, and therefore the fit will have large bias. Fig.7 shows examples of the resulting lineshape function for simulated, *in vitro* and *in vivo* signals.

When quantifying *in vitro* and *in vivo* signals, the approaches described in [27] present some limitations when denoising the lineshape function $g(t)$, such as too high outliers in the denoised lineshapes.

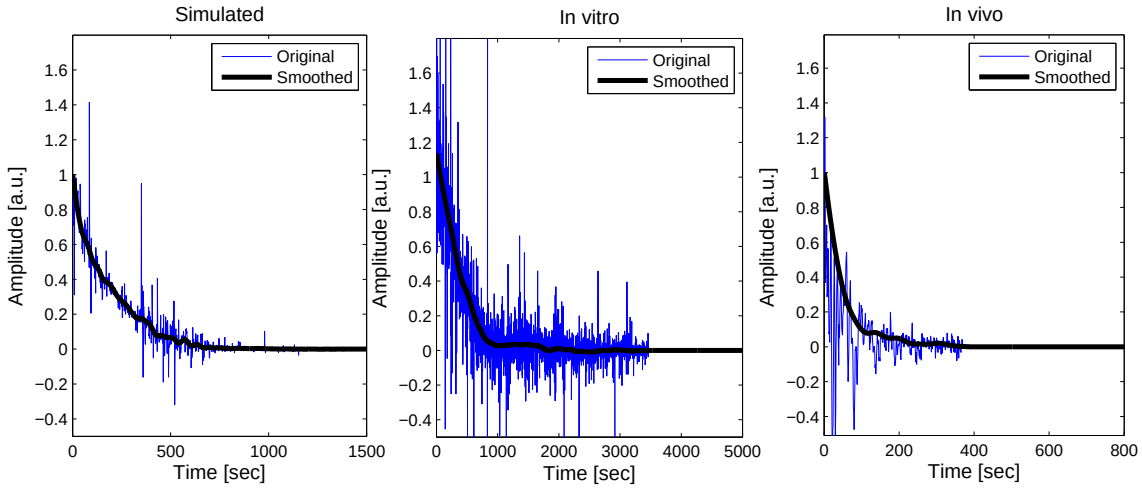

Figure 7: Time domain signal of the resulting lineshape for the simulated (left), *in vitro* (middle) and *in vivo* (right) signals. The original signal corresponds to the $g(t)$ function calculated with the ratio formula (6) and the smoothed signal is its final denoised version after convergence. The high signal variations seen in the middle plot are due to the division by small values in Eq.(6) of the ratio formula for $g(t)$.

Residual and other imperfections. When a quantification method like AQSES is used and a significant residual is observed after the estimation, several factors can be attributed to this problem. One of them is the lineshape distortion. However, incomplete metabolite basis set and spectral differences between the *in vivo* signal and the metabolite basis set, *e.g.* non-fitted peaks

due to temperature effects or chemical shift displacement errors (CSDE), may also cause an increase in the residual and thus an inaccurate quantification. To identify which of those factors is predominant in the estimation of metabolites is not obvious, however, it is recommended to choose the appropriate prior knowledge and consider the possible disturbances and external factors affecting the signals.

Potential imperfections could be such phase distortions due to J-modulation. With relatively short echo-times like in this study (TE= 20ms), only marginal phase errors might occur for functional groups with relatively large J-coupling constants (for example GABA, Glutamine, Glutamate or Myo-inositol with J up to 15Hz).

Additional 'ghost' echoes may be introduced in the signals caused by local gradients at tissue interferences. These echoes can be eliminated in the time domain by truncation of the last points where the echo is present. The use of navigator scans also track patient movements and potentially compensate for it. In AQSES Lineshape these kind of echoes are avoided when calculating the SNR for estimation of the cut-off point at which the signal is set to zero.

Background signals. *In vivo* short TE ^{1}H MRS signals are highly affected by an underlying signal of macromolecules and lipids. This problem can be solved either by estimating a background signal by means of non-parametric methods or by measuring it *in vivo* with a metabolite nulling procedure. This macromolecules/lipids signal (MM) can be added to the metabolite basis set used for the quantification. The most important drawback of measuring it *in vivo* is the time of acquisition, since the background signal can not be assumed to be similar for tissues affected by different diseases [26] and thus should be remeasured; moreover, it could contain residual metabolites. The time of measurement of MM depends on the acquisition parameters, thus the one used for our study takes about 45 minutes, while a normal MRS signal is measured in 15 minutes. If one does not acquire fully relaxed spectra, they could be acquired much faster (in the clinic this will be usually within 5 minutes for the normal MRS, and about 3 times more for the MM signal).

5 Conclusions

Accurate quantification of MRS signals is essential when clinical data need to be analyzed, therefore we consider the lineshape estimation an important step in the quantification of *in vivo* MRS signals and proposed an algorithm for it. We have illustrated difference in quantification with lineshape estimation on three scenarios of distorted MRS signals, namely on simulated, *in vitro* and *in vivo* signals. Asymmetric lineshape distortions with eddy current effects were considered in simulations, while mis-shimming was used to broaden and distort the measured *in vitro* and *in vivo* signals. Further work involves combination of the lineshape estimation algorithm with a background signal estimation using non-parametric methods and appropriate prior knowledge, which would circumvent the need for a time-consuming acquisition of macromolecular signals.

Acknowledgment

Maria I. Osorio Garcia and Dr. Flemming U. Nielsen are Marie Curie research fellows in the EU training network FAST (www.fast-mrs.eu). Dr. Diana M. Sima is a postdoctoral fellow of the Fund for Scientific Research-Flanders. Prof.Dr. Uwe Himmelreich and Prof.Dr.ir Sabine Van Huffel are full professors at the Katholieke Universiteit Leuven, Belgium.

Research supported by:

- Research Council KUL: GOA-AMBioRICS, GOA MaNet, CoE EF/05/006 Optimization in Engineering (OPTEC), IDO 05/010 EEG-fMRI, IDO 08/013 Autism, IOF-KP06/11 FunCopt, several PhD/postdoc & fellow grants;
- Flemish Government: FWO: PhD/postdoc grants, projects: FWO G.0302.07 (SVM), G.0341.07 (Data fusion), G.0427.10N (Integrated EEG-fMRI) research communities (ICCoS, ANMMM); IWT: TBM070713-Accelero, TBM070706-IOTA3, TBM080658-MRI (EEG-fMRI), PhD Grants;
- Belgian Federal Science Policy Office IUAP P6/04 (DYSCO, 'Dynamical systems, control and optimization', 2007-2011); ESA PRODEX No 90348 (sleep homeostasis)
- EU: FAST (FP6-MC-RTN-035801), Neuromath (COST-BM0601)

- K.U. Leuven Center of Excellence “MoSAIC”

References

[1] R. Bartha, D.J. Drost, R.S. Menon, and P.C. Williamson. Spectroscopic lineshape correction by QUECC: combined QUALITY deconvolution and eddy current correction. *Magn. Reson. Med.*, 44(4):641 – 645, 2000.

[2] A.M. Blamire, D.L. Rothman, and T. Nixon. Dynamic shim updating: a new approach towards optimized whole brain shimmings. *Magn. Reson. Med.*, 36(1):159 – 165, 1996.

[3] P.A. Bottomley. Selective volume method for performing localized NMR spectroscopy. *in U.S patent*, (4 480 228), 1984.

[4] W.S. Cleveland. Robust locally weighted regression and smoothing scatterplots. *J. Am. Stat. Assoc.*, 74(368):829–836, 1979.

[5] J.C. Cobas, M.A. Bernstein, M. Martín-Pastor, and P. García Tahoces. A new general-purpose fully automatic baseline-correction procedure for 1D and 2D NMR data. *J. Magn. Reson.*, 183(1):145 – 151, 2006.

[6] C. Cudalbu, V. Mlynarik, L. Xin, and R. Gruetter. Quantification of *in vivo* short echo-time proton magnetic resonance spectra at 14.1 T using two different approaches of modelling the macromolecule spectrum. *Meas. Sci. Technol.*, 20(10):104034 (7pp), 2009.

[7] Z. Dong and B.S. Peterson. Spectral resolution amelioration by deconvolution (SPREAD) in MR spectroscopic imaging. *J. Magn. Reson. Imaging*, 29(6):1395–1405, 2009.

[8] R. Gruetter. Automatic localized *in vivo* adjustment of all first- and second- order shim coils. *Magn. Reson. Med.*, 29(6):804–811, 1993.

[9] R. Gruetter, S.A. Weisdorf, V. Rajanayagan, M. Terpstra, H. Merkle, C.L. Truwit, M. Garwood, S.L Nyberg, and K. Ugurbil. Resolution improvements in in vivo ^{1}H NMR spectra with increased magnetic field strength. *J. Magn. Reson.*, 135(1):260–264, 1998.

[10] C. Juchem, B. Muller-Bierl, F. Schick, N.K. Logothetis, and J. Pfeuffer. Combined passive and active shimming for *in vivo* MR spectroscopy at high magnetic fields. *J. Magn. Reson.*, 183(2):278 – 289, 2006.

[11] C. Juchem, T.W. Nixon, S. McIntyre, D.L. Rothman, and R.A. de Graaf. Magnetic field homogenization of the human prefrontal cortex with a set of localized electrical coils. *Magn. Reson. Med.*, 63(1):171–180, 2010.

[12] U. Klose. In vivo proton spectroscopy in presence of eddy currents. *Magn. Reson. Med.*, 14(1):26 – 30, 1990.

[13] J. Knight-Scott. Application of multiple inversion recovery for suppression of macromolecule resonances in short echo time ^{1}H NMR spectroscopy of human brain. *J. Magn. Reson.*, 140(1):228 – 234, 1999.

[14] R. Kreis. Issues of spectral quality in clinical 1h-magnetic resonance spectroscopy and a gallery of artifacts. *NMR Biomed.*, 17(6):361 – 381, 2004.

[15] T. Laudadio, N. Mastronardi, L. Vanhamme, P. Van Hecke, and S. Van Huffel. Improved Lanczos algorithms for blackbox MRS data quantitation. *J. Magn. Reson.*, 157(2):292 – 297, 2002.

[16] J.S. Lee and D.D. Cox. Robust smoothing: Smoothing parameter selection and applications to fluorescence spectroscopy. *Comput. Stat. Data. An.*, 54(12):3131 – 3143, 2009.

[17] A.A. Maudsley. Spectral lineshape determination by self-deconvolution. *J. Magn. Reson.*, 106(1):47 – 57, 1995.

[18] K.R. Metz, M.M. Lam, and A.G. Webb. Reference deconvolution: A simple and effective method for resolution enhancement in Nuclear Magnetic Resonance Spectroscopy. *Concepts Magn. Reson.*, 12(1):21–42, 2000.

[19] J. Pfeuffer, I. Tkáč, S.W. Provencher, and R. Gruetter. Toward an *in vivo* neurochemical profile: Quantification of 18 metabolites in short-echo-time 1H NMR spectra of the rat brain. *J. Magn. Reson.*, 141(1):104 – 120, 1999.

[20] E. Popa, E. Capobianco, R. de Beer, D. van Ormondt, and D. Graveron-Demilly. *In vivo* quantitation of metabolites with an incomplete model function. *Meas. Sci. Technol.*, 20(10):104032 (9pp), 2009.

[21] J-B Poullet, D.M. Sima, A.W. Simonetti, B. De Neuter, L. Vanhamme, P. Lemmerling, and S. Van Huffel. An automated quantitation of short echo time MRS spectra in an open source software environment: AQSES. *NMR Biomed.*, 20(5):493 – 504, 2007.

[22] J-B Poullet, D.M. Sima, and S. Van Huffel. MRS signal quantitation: A review of time- and frequency-domain methods. *J. Magn. Reson.*, 195(2):134 – 144, 2008.

[23] S.W. Provencher. Estimation of metabolite concentrations from localized *in vivo* proton NMR spectra. *Magn. Reson. Med.*, 30(6):672–679, 1993.

[24] S.W. Provencher. Automatic quantitation of localized in vivo 1H spectra with LCModel. *NMR Biomed.*, 14(4):260–264, 2001.

[25] H. Ratiney, Y. Coenradie, S. Cavassila, D. van Ormondt, and D. Graveron-Demilly. Time-domain quantitation of 1H short echo-time signals: background accommodation. *MAGMA*, 16(6):284 – 296, 2004.

[26] U. Seeger, U. Klose, I. Mader, W. Grodd, and T. Naegele. Parameterized evaluation of macromolecules and lipids in proton MR spectroscopy of brain diseases. *Magn. Reson. Med.*, 49(1):19 – 28, 2003.

[27] D.M. Sima, M.I. Osorio-Garcia, J-B Poullet, A. Suvichakorn, J-P Antoine, S. Van Huffel, and D. van Ormondt. Lineshape estimation for MRS signals: self-deconvolution revisited. *Meas. Sci. Technol.*, 20(10):104031 (12pp), 2009.

[28] J. Slotboom, C. Boesch, and R. Kreis. Versatile frequency domain fitting using time domain models and prior knowledge. *Magn. Reson. Med.*, 39(6):899–911, 1998.

[29] S.A. Smith, T.O. Levante, B.H. Meier, and R.R. Ernst. Computer simulations in magnetic resonance. An object-oriented programming approach. *J. Magn. Reson.*, 106(1):75–105, 1994.

[30] D. Stefan, F. Di Cesare, A. Andrasescu, E. Popa, A. Lazariev, E. Vescovo, O. Strbak, S. Williams, Z. Starcuk, M. Cabanas, D. van Ormondt, and D. Graveron-Demilly. Quantitation of magnetic resonance spectroscopy signals: the jMRUI software package. *Meas. Sci. Technol.*, 20(10):104035(9pp), 2009.

[31] I. Tkáč, Z. Starčuk, I-Y. Choi, and R. Gruetter. *In vivo* ^{1}H NMR spectroscopy of rat brain at 1ms echo time. *Magn. Reson. Med.*, 41(4):649–656, 1999.

[32] P. Webb, D. Spielman, and A. Macovski. Inhomogeneity correction for in vivo spectroscopy by high-resolution water referencing. *Magn. Reson. Med.*, 23(1):1 – 11, 1992.